8. Fan H-j. Advances in pathogenesis of *Streptococcus suis* serotype 2. Journal of Integrative Agriculture. 2017;16: 2834–47.
9. Nicholson TL, Waack U, Anderson TK, Bayles DO, Zaia SR, Goertz I, et al. Comparative virulence and genomic analysis of *Streptococcus suis* isolates. Front Microbiol. 2021;11:620843. https://doi.org/10.3389/fmicb.2020.620843
10. Shapiro M, Walker M, Carroll KT, Levitt MR, Raz E, Nossek E, et al. Neuroanatomy of cranial dural vessels: implications for subdural hematoma embolization. J Neurointerv Surg. 2021;13:471–7. https://doi.org/10.1136/neurintsurg-2020-016798

Address for correspondence: Eui Tae Kim or Jong-Kook Rhim, Jeju National University College of Medicine, Aran 13gil 15 (Ara-1 Dong) Jeju-si, Jeju Self-Governing Province, 63241, South Korea; email: tae@jejunu.ac.kr or nsrhim@gmail.com

Incursion of Highly Pathogenic Avian Influenza A(H5N1) Clade 2.3.4.4b Virus, Brazil, 2023

Andreina Carvalho de Araújo,[1] Laura Morais Nascimento Silva,[1] Andrew Yong Cho,[1] Márcio Repenning, Deyvid Amgarten, Ana Paula de Moraes, Fernanda Malta, Michael Miller, Erick G. Dorlass, Soledad Palameta, Daniele Bruna L. Oliveira, Jansen de Araújo, Clarice Weis Arns, Edison L. Durigon, João Renato R. Pinho, Dong-Hun Lee, Helena Lage Ferreira

Author affiliations: University of São Paulo, Pirassununga, Brazil (A.C. Araujo, L.M.N. Silva, D.B.L. Oliveira, J. De Araujo, E.L. Durigon, J.R.R. Pinho, H.L. Ferreira); Konkuk University, Gwangjin-gu, South Korea (A.Y. Cho, D.-H. Lee); FURG, Rio Grande, Brazil (M. Repenning); Albert Einstein Israelite Hospital, São Paulo, Brazil (D. Amgarten, F. Malta, E.G. Dorlass, D.B.L. Oliveira, J.R.R. Pinho); UNICAMP, Campinas, Brazil (A.P. de Moraes, M. Miller, S. Palameta, C.W. Arns); Institut Pasteur, São Paulo, Brazil (E.L. Durigon)

DOI: http://doi.org/10.3201/eid3003.231157

[1]These authors contributed equally to this article.

We report 4 highly pathogenic avian influenza A(H5N1) clade 2.3.4.4.b viruses in samples collected during June 2023 from Royal terns and Cabot's terns in Brazil. Phylodynamic analysis revealed viral movement from Peru to Brazil, indicating a concerning spread of this clade along the Atlantic Americas migratory bird flyway.

Highly pathogenic avian influenza viruses (HPAIVs) have caused substantial economic losses in the poultry industry and potentially threaten public health. Since its first identification in 1996, H5Nx HPAIVs, Gs/GD lineage, have evolved into multiple genotypes through reassortment across decades (*1*–*3*).

In late 2020, novel reassortant clade 2.3.4.4b H5N1 HPAIVs emerged and became predominant in Europe (*1*). The first detection of clade 2.3.4.4 b H5N1 viruses in North America occurred through transatlantic spread via wild birds in late 2021 (*2*). From late 2021 to early 2022, multiple reassortant viruses have been naturally generated by recombination with North American low pathogenicity avian influenza virus (LPAIV) internal genes. In late October 2022, South America countries including Argentina, Bolivia, Brazil, Chile, Colombia, Ecuador, Paraguay, Peru, Uruguay, and Venezuela reported clade 2.3.4.4 b H5N1 HPAIV detection in domestic and wild birds (*3*,*4*). Human infections were also reported for the first time in South America (*3*,*5*). We report 4 clade 2.3.4.4b H5N1 HPAIVs sequenced from wild bird carcasses collected in Brazil in June 2023.

In June 2023, we collected swab samples from Royal terns (*Thalasseus maximus*) and Cabot's terns (*Thalasseus acuflavidus*) in Brazil, from which we detected and sequenced 4 H5N1 HPAIVs: A/Thalasseus_maximus/Brazil-ES/23ES1A0008/2023 (TM/BR08/23), A/Thalasseus_acuflavidus/Brazil-ES/23ES1A0009/2023 (TA/BR09/23), A/Thalasseus acuflavidus/Brazil-ES/23ES1A0025/2023 (TA/BR25/23), and A/Thalasseus maximus/Brazil-ES/23ES1A0026/2023 (TM/BR26/23) (Appendix 1, https://wwwnc.cdc.gov/EID/article/30/3/23-1157-App1.pdf). We obtained complete genome sequences for TM/BR08/23 and TM/BR09/23 and partial sequences for TA/BR25/23 and TM/BR26/23 (GISIAD [https://www.gisaid.org] accession nos. EPI_ISL_18130597, EPI_ISL_18130622, EPI_ISL_18130627, and EPI_ISL_18130628) (Appendix 1 Table 1).

All H5N1 isolates possessed polybasic amino acid sequences at the hemagglutinin (HA) cleavage site (PLREKRKKR/GLF). The isolates shared high sequence identities (99.59%–100%) across all 8 genes. BLAST search (https://blast.ncbi.nlm.nih.gov) showed all 8 genes shared high identities (99.59%–

100%) to the recent H5N1 HPAIVs isolated from samples obtained in Chile and other South American countries. Using maximumplikelihood phylogenies, we noted that all internal genes (polymerase basic [PB] 2, PB1, polymerase acidic [PA], nucleoprotein [NP], matrix [M], nonstructural [NS]) clustered with the B3.2 genotype, a reassortant genotype identified in the United States in early 2022. The B3.2 genotype comprises North America–origin PB2, PB1, NP, and NS and Eurasia–origin PA, HA, NA, and M. We observed no evidence of reassortment, indicating the viruses were direct descendants of genotype B3.2 (Appendix 1 Figure 1) (*6*). Bayesian phylogeny of the HA gene revealed the H5N1 viruses from Brazil formed a well-supported cluster. We estimated the time to most recent ancestor to be May 13, 2023 (95% highest posterior density April 15, 2023–June 10, 2023), suggesting the H5N1 HPAIVs emerged ≈1 month before the detection in the carcasses of wild terns (Figure).

We estimated the incursion of genotype B3.2 into South America to be around August 14, 2022 (95% highest posterior density July 3, 2022–September 21 2022). Discrete trait analysis of geographic location suggested the source of H5N1 HPAIV was from North America, with frequently observed viral movement from Peru to Chile (Figure). The viral transition from Chile to Brazil was highly supported. However, the long branch between the two countries suggests a lack of data to be filled (Figure; Appendix 1 Tables 2, 3). Discrete trait analysis after minimizing the sampling bias showed similar results to the initial analysis (Appendix 1 Figure 2).

We evaluated mammalian molecular markers by using the H5N1 HPAIVs and the human virus from Chile (A/Chile/25945/2023) (*5*). The HA protein sequences of the H5N1 HPAIVs had amino acids related to those with a binding affinity to avian-like (α-2,3 sialic acid) receptors (188T, 210A, 222Q, and 224G in H5 numbering) (*7*,*8*). The HA protein sequences had 3 minor substitutions associated with increased binding affinity of the HA receptor to a human-like receptor (α-2,6 sialic acid) (S123P, S133A, and T156A in HA) (Appendix 1 Table 4). All isolates exhibited L89V, K389R, and V598T in PB2; N30D, I43M, and T215A in M; and P42S and ESEV PDZ binding motif mutations in NS, known to increase virulence in mice. The Chilean virus harbored more amino acid substitutions known to be associated with increased viral replication in mammals, including Q591K and D701N in PB2, A515T in PA, and L98F and I101M in NS (Appendix 1 Table 4).

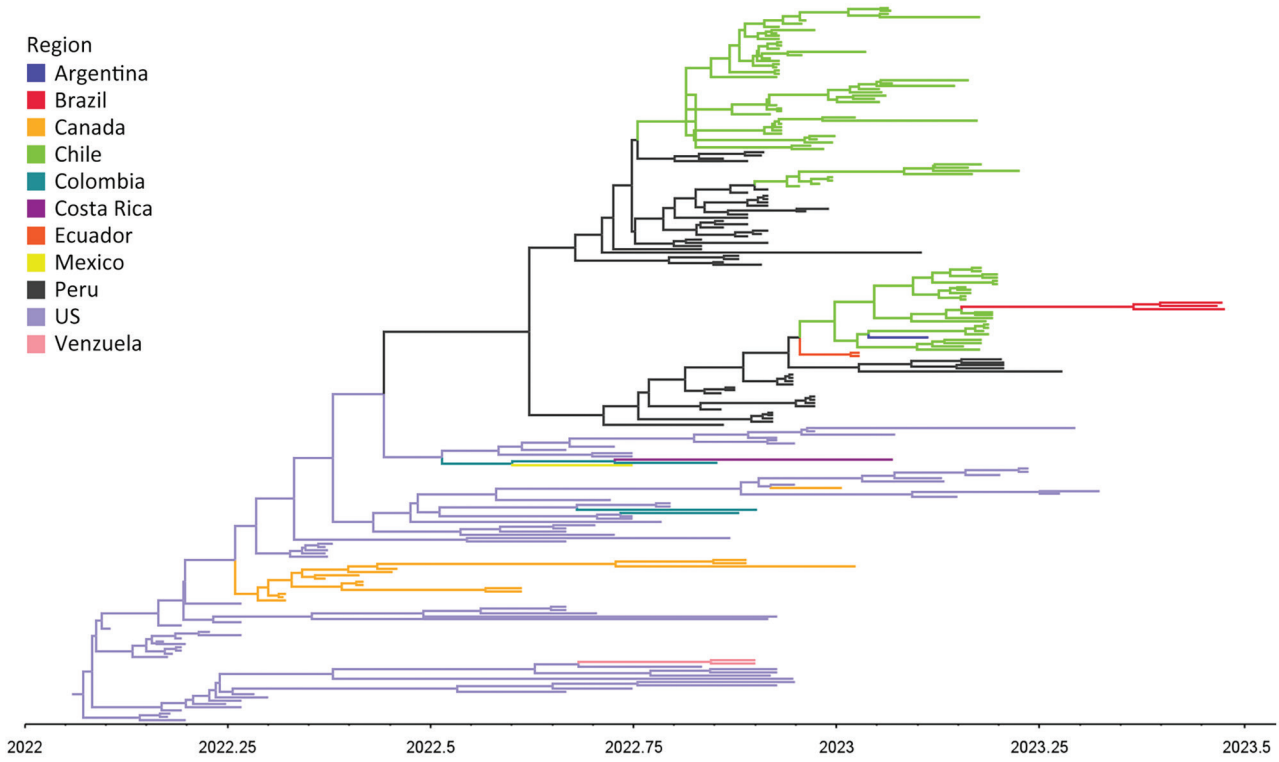

Figure. Maximum clade credibility phylogenetic tree of hemagglutinin gene based on discrete trait analysis of geographic location of wild bird carcasses identified as harboring highly pathogenic avian influenza A(H5N1) clade 2.3.4.4b virus, Brazil, 2023. The time scale is shown on the horizontal axis. Each branch is colored according to geographic region.

The reassortment of H5Nx clade 2.3.4.4b HPAIVs, containing segments from both HPAIVs and LPAIVs, created a diverse genetic pool of H5 clade 2.3.4.4 that is continuously emerging in various countries (*9*). Novel reassortment of Eurasian clade 2.3.4.4 HPAIV with North America LPAIVs was reported in 2014–2015 and 2022–2023 (*6*,*10*). South America has been largely unaffected by the HPAIV epizootic in the past decade, but more countries are reporting HPAIV since its first detection in October 2022. Royal terns and Cabot's terns are mainly coastal birds, staying on shore areas all year (P. Yorio et al., unpub. data, https://doi.org/10.1675/1524-4695-31.4.561). The terns are known to use the Atlantic Americas Flyway and move along the coast, which raises concern for the spread of H5N1 HPAIV in this region. The unprecedented global distribution and continuous generation of novel reassortant clade 2.3.4.4b HPAI H5Nx viruses call for heightened monitoring of HPAIV movement and reassortment to improve prevention and control policies.

Acknowledgments

The authors gratefully acknowledge Julia Cristina Benassi Bueno and Alessandra Greatti for their technical assistance and Cristian M. Joenck for fieldwork assistance. We thank the support of the Brazilian Post and Telegraph Company (Correios) for transporting our fieldwork supplies and samples. We also thank the National Network for Virus Surveillance in Wild Animals (PREVIR Network). We gratefully acknowledge all data contributors (i.e., the authors and their originating laboratories responsible for obtaining the specimens and their submitting laboratories) for generating the genetic sequence and metadata and sharing via GISAID (https://www.gisaid.org), on which this research is based (Appendix 2, https://wwwnc.cdc.gov/EID/article/30/3/23-1157-App2.xlsx).

This work is funded by the Ministry of Science, Technology, and Innovation (MCTI-Brazil) and by the National Council for Scientific and Technological Development (CNPq: 403761/2020-4, 400172/2022-4, and 405786/2022-0). A.G., H.L.F., and C.W.A. are recipients of the CNPq scholarship. L.M.N.S. is the recipient of the CAPES scholarship.

About the Author

Dr. Araujo is a veterinarian and postdoctoral fellow at the University of São Paulo, Brazil. Her research focuses on the epidemiology and diagnosis of infectious and parasitic diseases.

References

1. Pohlmann A, King J, Fusaro A, Zecchin B, Banyard AC, Brown IH, et al. Has epizootic become enzootic? evidence for a fundamental change in the infection dynamics of highly pathogenic avian influenza in Europe, 2021. MBio. 2022;13:e0060922. https://doi.org/10.1128/mbio.00609-22
2. Caliendo V, Lewis NS, Pohlmann A, Baillie SR, Banyard AC, Beer M, et al. Transatlantic spread of highly pathogenic avian influenza H5N1 by wild birds from Europe to North America in 2021. Sci Rep. 2022;12:11729. https://doi.org/10.1038/s41598-022-13447-z
3. Adlhoch C, Fusaro A, Gonzales JL, Kuiken T, Melidou A, Mirinavičiūtė G, et al; European Food Safety Authority, European Centre for Disease Prevention and Control, European Union Reference Laboratory for Avian Influenza. Avian influenza overview, April–June 2023. EFSA J. 2023;21:e08191.
4. World Organisation for Animal Health. World Animal Health Information System (WAHIS) Events Management. Search: High pathogenicity avian influenza viruses (poultry) and South American countries. Accession date 2023 Nov 7 [cited 2023 Nov 23]. https://wahis.woah.org/#/event-management
5. Castillo A, Fasce R, Parra B, Andrade W, Covarrubias P, Hueche A, et al. The first case of human infection with H5N1 avian Influenza A virus in Chile. J Travel Med. 2023;30:taad083. https://doi.org/10.1093/jtm/taad083
6. Youk S, Torchetti MK, Lantz K, Lenoch JB, Killian ML, Leyson C, et al. H5N1 highly pathogenic avian influenza clade 2.3.4.4b in wild and domestic birds: introductions into the United States and reassortments, December 2021–April 2022. Virology. 2023;587:109860. https://doi.org/10.1016/j.virol.2023.109860 PMID: 37572517
7. Suttie A, Deng YM, Greenhill AR, Dussart P, Horwood PF, Karlsson EA. Inventory of molecular markers affecting biological characteristics of avian influenza A viruses. Virus Genes. 2019;55:739–68. https://doi.org/10.1007/s11262-019-01700-z
8. Burke DF, Smith DJ. A recommended numbering scheme for influenza A HA subtypes. PLoS One. 2014;9:e112302. https://doi.org/10.1371/journal.pone.0112302
9. Gu M, Liu W, Cao Y, Peng D, Wang X, Wan H, et al. Novel reassortant highly pathogenic avian influenza (H5N5) viruses in domestic ducks, China. Emerg Infect Dis. 2011;17:1060–3. https://doi.org/10.3201/eid/1706.101406
10. Lee DH, Criado MF, Swayne DE. Pathobiological origins and evolutionary history of highly pathogenic avian influenza viruses. Cold Spring Harb Perspect Med. 2021;11:a038679. https://doi.org/10.1101/cshperspect.a038679

Address for correspondence: Helena Lage Ferreira, Department of Veterinary Medicine, FZEA-USP, University of São Paulo, 225 Av Duque de Caxias Norte, 13635900, Pirassununga, SP, Brazil; email: hlage@usp.br

Article DOI: http://doi.org/10.3201/eid3003.231157

EID cannot ensure accessibility for supplementary materials supplied by authors. Readers who have difficulty accessing supplementary content should contact the authors for assistance.

Incursion of Highly Pathogenic Avian Influenza A(H5N1) Clade 2.3.4.4b Virus, Brazil, 2023

Appendix

Methods and Materials

Ethics Statement

The authors confirm that the ethical policies of the journal, as noted on the journal's author guidelines page, have been adhered to and the appropriate ethical review committee approval has been received. All applicable international, national, and/or institutional guidelines for the care and use of animals were followed. Sample collections were authorized by the Brazilian Institute of Environment and Natural Renewable Resources (SISBIO/IBAMA: 64261-6), by the Ethics Committee on the Use of Animals of the University of São Paulo (CEUA/FZEA-USP: 1128141120), and National System for the Management of Genetic Heritage and Associated Traditional Knowledge (SISGEN A028CF5).

Virus Detection

Cloacal swab samples from wild birds were collected in the coastal region of Espírito Santo and close to the Estuary of the Doce River in June 2023. Eighty-one individuals belonging to 48 bird species from 23 orders were sampled. All of the animals captured were healthy, except five birds found dead in the environment without any clinical signs reported. The five carcasses belonged to two species (*Thalasseus acuflavidus and Thalasseus maximus*), *Charadriiformes* order. Total RNA was extracted using MagMax core nucleic acid purification kit (Thermofisher, California, USA) from swab samples according to the manufacturer's instructions. RNA was tested for influenza A virus matrix gene by real-time reverse transcription PCR (RT-qPCR) as previously described (*1*). Influenza A positive viruses were only detected from swab samples of

four carcasses of Royal tern (*Thallasseus maximus*) and Cabot's tern (*Thallasseus acuflavidus*). (Appendix 1 Table 1).

Full-genome sequencing and assembly

All 8 genes of each sample were amplified using the *SuperScript* IV *Reverse Transcriptase kit* (Thermo Fisher Scientific, USA) using the universal primers as previously described (*2*). Library preparation was done using the Nextera XT DNA kit (Illumina). Next generation sequencing was run on NextSeq 550 (Illumina, San Diego, California, USA) with NextSeq 500/550 Mid Output Kit v2 (300-cycles). AIV genome segment sequences were obtained by reference (segments from A/Gull/CHL/227023-3/2022(H5N1), BioProject: PRJNA323817) guided assembly using Geneious Prime software version 2023.2.1 (https://www.geneious.com). Number of reads per segment ranged from 148,373 to 497339 for TM/BR08/23, 97,425 to 305,070 for TM/BR09/23, 131996 to 832140 for TM/BR25/23, 175,542 to 474,714 for TM/BR26/23. All 8 genes from samples were uploaded in the EpiFlu database of Global Initiative on Sharing All Influenza Data (GISAID: https://www.gisaid.org), under the accession numbers: EPI_ISL_18130597 and EPI_ISL_18130622 (Complete genome was obtained for TM/BR08/23 and TM/BR09/23, respectively). EPI_ISL_18130627 and EPI_ISL_18130628 (AIV genome partially sequenced of TA/BR25/23 and TM/BR26/23, respectively) (Appendix 1 Table 1)

Phylogenetic Inference

GISAID Epiflu (https://platform.gisaid.org) database and NCBI BLAST database were used to retrieve the reference sequences for comparative phylogenetic analysis (*3*). Reference sequences were obtained based on sequence identity. ElimDupes software (https://www.hiv.lanl.gov/content/sequence/elimdupesv2/elimdupes.html) was used with sequence identity thresholds set at 99.5%-100% to subsample genomes from over-represented discrete sample location traits. Complete coding regions were aligned by using MAFFT (https://mafft.cbrc.jp/alignment/software/). We generated maximum-likelihood (ML) trees of each gene segment. We used the RAxML with general time-reversible (GTR) + gamma nucleotide substitution model and 1,000 rapid bootstrap replicates. Genotype of the virus genome were assigned using GenoFLU (https://github.com/USDA-VS/GenoFLU) (*4*). For further Bayesian discrete trait analysis, sequences were selected for optimal root-to-tip regression.

Using the combined dataset from GISAID Epiflu database and NCBI BLAST database, we performed Bayesian discrete trait analysis of 228 HA genes using BEAST v1.10.4 and applied an uncorrelated log-normal distribution relaxed clock method, the Hasegawa–Kishino–Yano + gamma nucleotide substitution model, and the Gaussian Markov random field Bayesian skyride coalescent prior. Markov Chain Monte Carlo method to sample trees and evolutionary parameters was run in quadruple 100 million chains (*5*). Four independent chains were combined for adequate sampling of the posterior distribution of trees. Convergence and effective sample size was analyzed with TRACER v1.4 (https://beast.bio.ed.ac.uk/tracer) with 10% burn-in. A maximum clade credibility (MCC) tree was generated by using TreeAnnotator v1.10.4 (http://www.phylo.org/index.php/tools/treeannotator.html) and visualized with FigTree v1.4.2 (https://tree.bio.ed.ac.uk/). Viral transmission between discrete traits was analyzed using the Bayesian stochastic search variable selection using SpreaD3 v0.9.7 software.

The Bayesian discrete trait phylogeography approach used in this study can be affected severely by under or over-represented numbers of sequences with respect to location states. The influence of sampling bias was assessed by location state randomization (*6*,*7*). The discrete states were randomly swapped throughout the Bayesian phylogeography analysis and the estimated root location state frequency of each discrete state was compared. The probability of the estimated ancestral root state of each discrete state should be similar in unbiased datasets when discrete traits are randomly swapped throughout the analysis. To minimize the effect of sampling bias, sequences were down-sampled by removing redundant sequences. The sequences from 4 over-represented discrete traits, Canada, USA, Chile, and Peru were down-sampled based on the sequence identity at 99.5-100% using the ElimDupes software and 3 discrete traits containing only single sequence (Costa Rica, Mexico, and Argentina) were excluded to ensure that every group has less than 20% of total number of sequences (Appendix 1 Table 2). The down-sampled dataset contained a total of 31 sequences.

Amino acid substitutions associated with viral adaptation in mammalian hosts

To examine amino acid changes associated with mammalian adaptation, we used HA Subtype Numbering Conversion from Bacterial and Viral Bioinformatics Resource Center (https://www.bv-brc.org/) to align HA sequences from this study into H5 numbering scheme (8). Internal gene sequences were aligned using MAFFT (http://mafft.cbrc.jp/alignment/software/).

Results

For the complete data set, the root location state frequencies of discrete states were not evenly distributed (0.01-39.01%) when discrete traits were randomly swapped throughout the analysis, indicating a strong impact of sample size in this data set (Appendix 1 Table 2). The Chile category had the highest root location state frequency (59.01%) which is most likely influenced by the large number of samples in this discrete state. To reduce this bias, the data set was additionally down-sampled to have more balanced sample sizes. For the down-sampled data set, the root location state frequency of each discrete state was more similar (7.04-21.27%) to each other than that of original dataset, indicating a low impact of sample size in this analysis. The phylogeography analysis using the down-sampled data set showed identical pattern of virus transmissions with the complete dataset (Appendix 1 Table 3). Despite uneven sample size in the complete data set, both analyses showed identical migration pattern of virus, suggesting the discrete trait analysis results of complete dataset adequately represent the overall transmission routes of virus. Additionally, Brazilian 2.3.4.4b H5N1 HPAIV sequences contain amino acid residues known to be associated with increased virulence in mammals (Appendix 1 Table 4). Our data presents the most probable transmission routes using all available data, and the results strongly indicate the virus spread from USA to Brazil through Peru and Chile.

References

1. Spackman E, Senne DA, Bulaga LL, Myers TJ, Perdue ML, Garber LP, et al. Development of real-time RT-PCR for the detection of avian influenza virus. Avian Dis. 2003;47(Suppl):1079–82. PubMed https://doi.org/10.1637/0005-2086-47.s3.1079

2. Lee DH. Complete Genome Sequencing of Influenza A Viruses Using Next-Generation Sequencing. Methods Mol Biol. 2020;2123:69–79. PubMed https://doi.org/10.1007/978-1-0716-0346-8_6

3. Shu Y, McCauley J. GISAID: Global initiative on sharing all influenza data - from vision to reality. Euro Surveill. 2017;22:30494. PubMed https://doi.org/10.2807/1560-7917.ES.2017.22.13.30494

4. Youk S, Torchetti MK, Lantz K, Lenoch JB, Killian ML, Leyson C, et al. H5N1 highly pathogenic avian influenza clade 2.3.4.4b in wild and domestic birds: Introductions into the United States and reassortments, December 2021–April 2022. Virology. 2023;587:109860.

5. Suchard MA, Weiss RE, Sinsheimer JS. Bayesian selection of continuous-time Markov chain evolutionary models. Mol Biol Evol. 2001;18:1001–13. PubMed https://doi.org/10.1093/oxfordjournals.molbev.a003872

6. Edwards Ceiridwen J, Suchard Marc A, Lemey P, Welch John J, Barnes I, Fulton Tara L, et al. Ancient Hybridization and an Irish Origin for the Modern Polar Bear Matriline. Current Biology. 2011;21(15):1251-8.

7. Hicks JT, Dimitrov KM, Afonso CL, Ramey AM, Bahl J. Global phylodynamic analysis of avian paramyxovirus-1 provides evidence of inter-host transmission and intercontinental spatial diffusion. BMC Evolutionary Biology. 2019;19(1):108.

8. Burke DF, Smith DJ. A recommended numbering scheme for influenza A HA subtypes. PLoS One. 2014;9:e112302. PubMed https://doi.org/10.1371/journal.pone.0112302

Appendix Table 1. Clade 2.3.4.4 b H5N1 high pathogenicity avian influenza virus isolated in this study.

ID	Subtype	Collection Date	Species identified	Location	RT-qPCR M gene (Ct)	GISAID ID
TM/BR08/23	H5N1	2023-06	Royal tern	Espirito Santo	Positive (28.57)	EPI_ISL_18130597
TA/BR09/23	H5N1	2023-06	Cabot's tern	Espirito Santo	Positive (22.51)	EPI_ISL_18130622
TA/BR25/23	H5N1	2023-06	Cabot's tern	Espirito Santo	Positive (20.69)	EPI_ISL_18130627
TM/BR26/23	H5N1	2023-06	Royal tern	Espirito Santo	Positive (28.67)	EPI_ISL_18130628

Appendix Table 2. Number of sequences in each discrete state and root location state frequency estimates result from location state randomization analysis.

	Number of sequences and root location state frequency (%) of each discrete state			
	Complete dataset (n=228)		Down-sampled dataset (n=31)	
Discrete state	Number of sequences (%)	Root location state frequency	Number of sequences (%)	Root location state frequency (%)
Chile	77 (33.8%)	59.03%	5 (16.1%)	13.58%
USA	72 (31.6%)	39.01%	6 (19.4%)	14.10%
Peru	51 (22.4%)	0.01%	6 (19.4%)	18.47%
Canada	15 (6.6%)	1.32%	4 (12.9%)	21.27%
Brazil	3 (1.3%)	0.19%	3 (9.7%)	7.04%
Colombia	3 (1.3%)	0.21%	3 (9.7%)	11.00%
Venezuela	2 (0.9%)	0.03%	2 (6.5%)	7.18%
Ecuador	2 (0.9%)	0.04%	2 (6.5%)	7.36%
Argentina	1 (0.4%)	0.01%	-	-
Costa Rica	1 (0.4%)	0.07%	-	-
Mexico	1 (0.4%)	0.08%	-	-

Appendix Table 3. 2.3.4.4b H5N1 HPAIV transmission matrix of Bayesian stochastic search variable selection analysis of geographic location

Dataset	From	To	Bayes factor	Posterior Probability
Complete (n=228)	USA	Canada	30387.8	1.00
	Peru	Chile	18566.7	1.00
	USA	Columbia	4700.1	1.00
	Chile	Brazil	194.1	0.95
	Peru	Ecuador	119.3	0.93
	Chile	Argentina	87.6	0.90
	USA	Venezuela	51.0	0.85
	USA	Peru	41.7	0.82
	Colombia	Costa Rica	13.2	0.59
	Colombia	Mexico	9.5	0.50
Down-sampled (n=31)	Peru	Chile	1196.3	0.99
	Chile	Brazil	126.4	0.95
	USA	Columbia	98.4	0.94
	Peru	Ecuador	28.9	0.82
	USA	Canada	12.0	0.66
	USA	Venezuela	11.6	0.65
	USA	Peru	5.9	0.50

Appendix Table 4. Amino acid substitutions of Brazilian 2.3.4.4b H5N1 HPAIV, June 2023. Sequences with amino acid residues known to be associated with increased virulence in mammals were highlighted in pink.

	HA (H5 numbering) *									PB2†					PA‡	NP#		M1§			NS**				
Isolates	D94N	S123P	S133A	N154D	T156A	T188I	V210I	Q222L	G224S	L89V	D256G	Q591K	E627K	D701N	A515T	Y52NQH	F313Y	N30D	I43M	T215A	P42S	80-84 deletion	L98F	I101M	ESEV
Brazil isolates	S	P	A	N	A	T	A	Q	G	V	D	Q	E	D	D	Y	F	D	M	A	S	TIASV	M	D	ESEV
A/Chile/25945/2023	S	P	A	N	A	T	A	Q	G	V	D	K	E	N	T	Y	F	D	M	A	S	TIASV	F	M	ESEV

* D94N, S123P, S133A, N154DN154D, T156A, T188I, V210I, Q222L, and G224S mutations in HA are known to be associated with increased binding to human-like receptor (α-2,6 sialic acid).
† L89V and D256G mutations in PB2 are known to be associated with increased virulence in mice. Q591K, E627K, and D701N mutations in PB2 are known to be associated with increased viral replication in mammals.
‡ A515T mutation in PA is known to be associated with H5 transmissibility in ferrets.
# Y52NQH and F313Y is known to be associated with human BTN3A3 evasion
§ N30D, I43M, T215A mutations in M1 are known to be associated with increased virulence in mice.
** P42S, 80-84 deletion, and ESEV PDZ binding motif mutations in NS are known to be associated with increased virulence in mice.

Appendix Figure 1 (see following pages). Maximum-likelihood phylogenetic tree using eight genes of H5N1 HPAIV: A) PB2, B) PB1, C) PA, D) HA, E) NP, F) NA, G) MP, and H) NS. Node values represent bootstrap values. Tips of Brazilian isolates are labeled in red. Branches of South American isolates are highlighted in yellow shade. Scale bar indicates nucleotide substitutions per site.

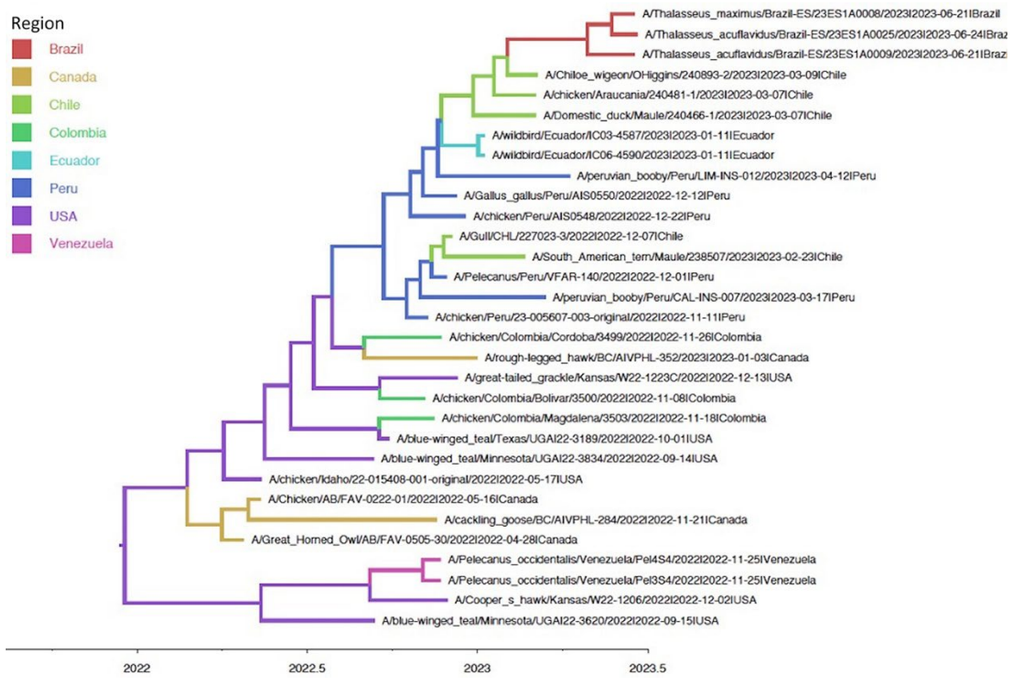

Appendix Figure 2. Bayesian phylogenetic maximum clade credibility (MCC) tree using the down-sampled data set of the clade 2.3.4.4b H5N1 HPAIVs. Branches are colored according to discrete traits of geographic regions. The scale axis indicates the branch length by year.

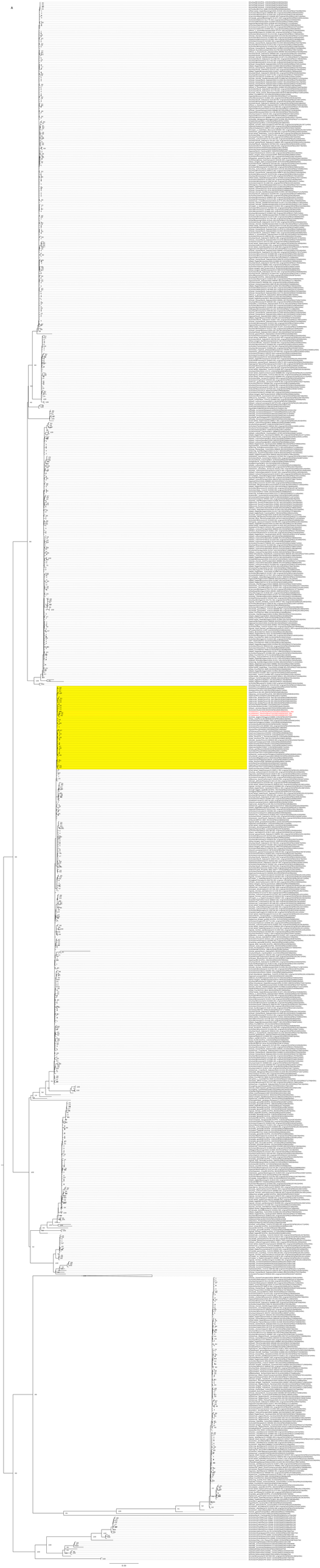
A
0.01

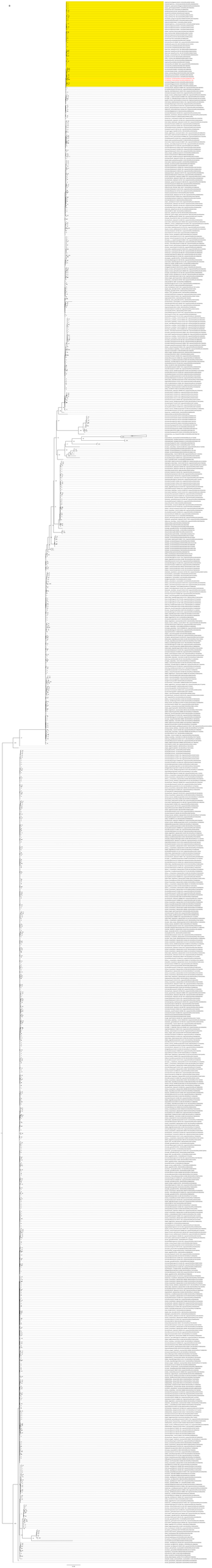

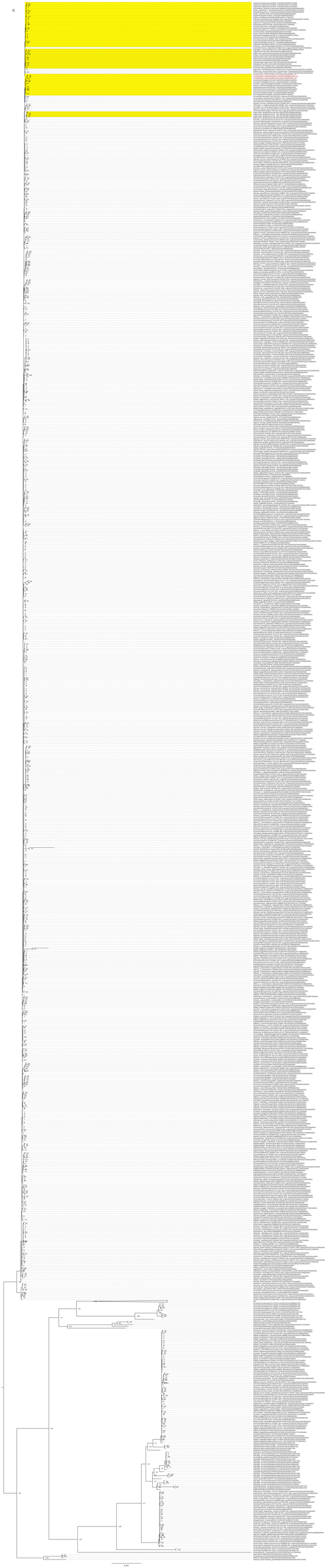
C
0.03

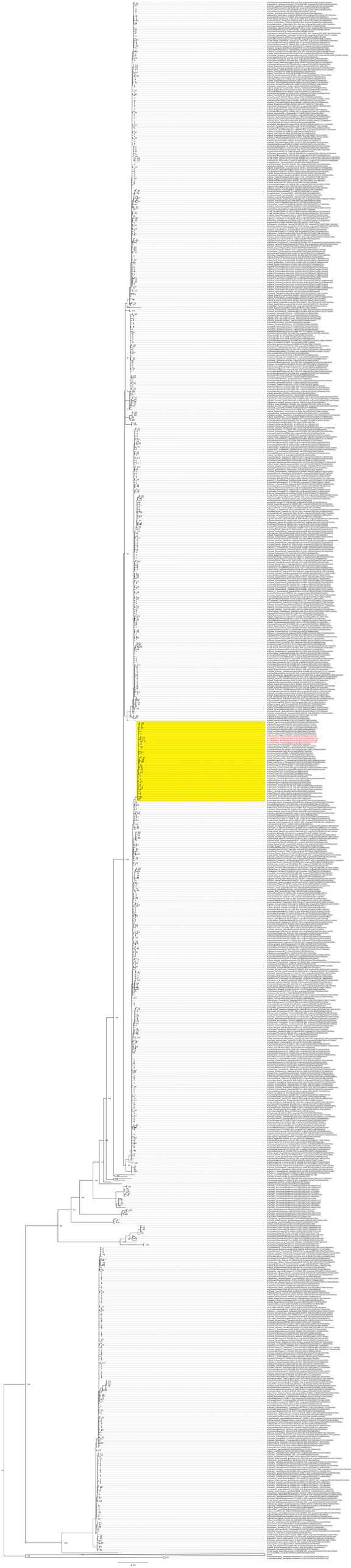
0.01

[redacted]

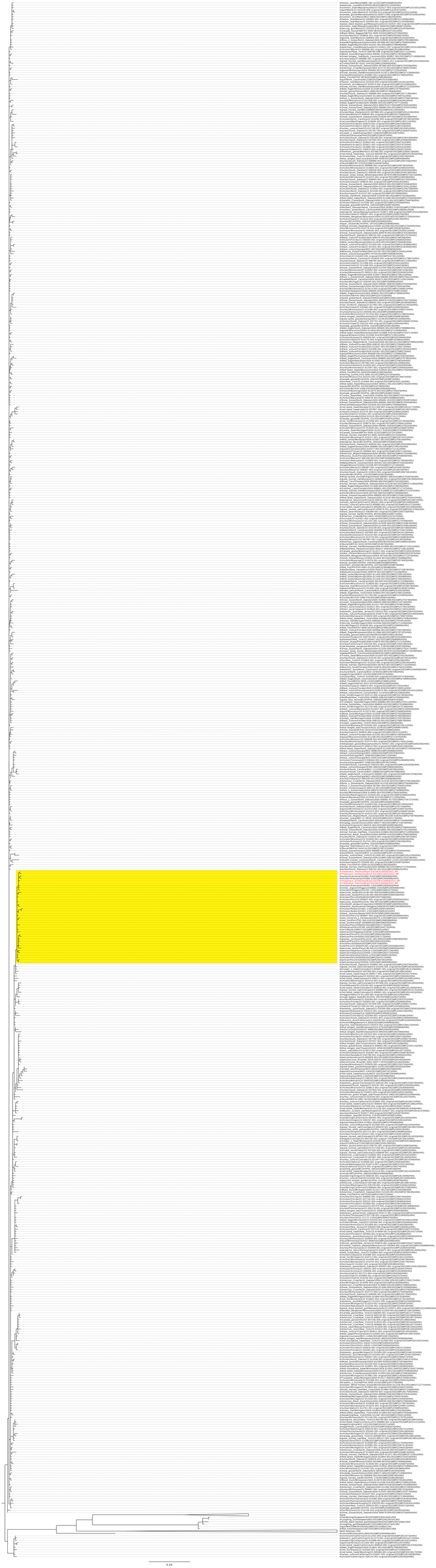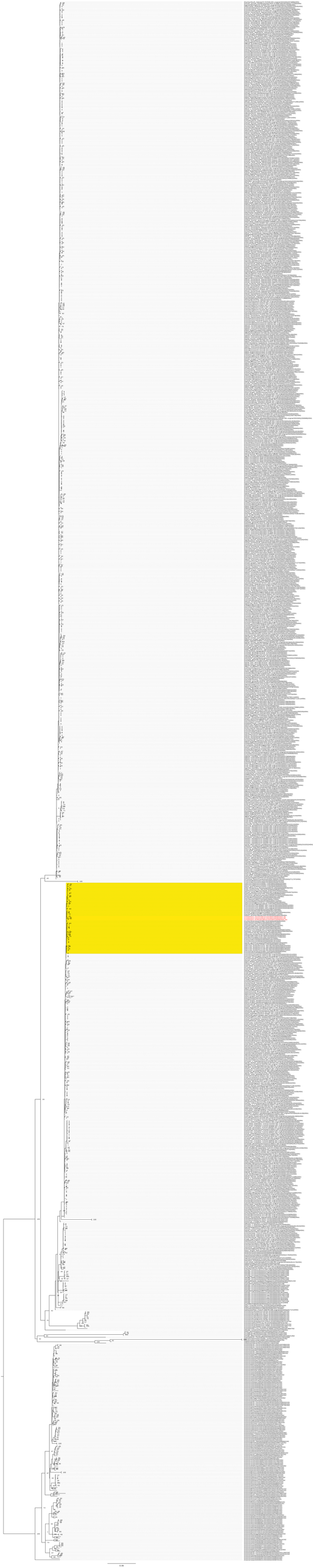
0.03